Influence of polydispersity on the effective interaction in a quasi-two-dimensional pseudo-one-component colloid fluid

Derek Frydel and Stuart A. Rice
Department of Chemistry and The James Franck Institute, The University of Chicago, Chicago, Illinois 60637, USA
(Received 1 October 2004; revised manuscript received 7 January 2005; published 13 April 2005)

We report the results of simulations of one-component and binary quasi-two-dimensional polydisperse hard sphere colloid fluids. When the polydisperse one-component system is regarded as an effective monodisperse one-component system, our results show that polydispersity gives rise to effective pair attraction and soft repulsion. These effective interactions depend on both the degree of polydispersity and the system density. At low density only the effective soft repulsion survives and the effective attraction becomes negligible. For the binary system, the depletion interaction develops extra features due to polydispersity, specifically a repulsive interaction with range twice the average particle diameter. At low density this extra feature vanishes. To carry out our study we have devised a method for continuous sampling of the polydisperse mixture according to a prescribed particle diameter distribution.

DOI: 10.1103/PhysRevE.71.041403 PACS number(s): 82.70.Dd, 61.20.Ja, 61.20.Lc, 66.30.−h

I. INTRODUCTION

There has been considerable recent interest in the equilibrium and dynamical properties of colloid systems. In part this interest is driven by the need to understand colloid system behavior and in part by the isomorphism (derived from the McMillan-Mayer theory [1]) between the equilibrium properties of a colloid assembly and an atomic system in the same state of aggregation. The latter permits use of the colloid system as a surrogate for the atomic system. One example of the use of that isomorphism is the study of the effect of dimensionality on structure and on transitions between structures, in particular the behavior in the quasi-two-dimensional (Q2D) limit [2]. Advances in experimental technique, notably digital video microscopy, provide a means to visualize the time dependences of colloid particle trajectories, from which the equilibrium structure and equilibrium distribution functions, as well as various time correlation functions characterizing the particle motion, can be calculated. Using well-established procedures, the effective colloid-colloid interaction can then be inferred by inversion of the experimentally determined pair correlation function.

The validity of the calculation of the effective colloid-colloid interaction depends on the accuracy of the assumption that the colloid particles are identical, as would be the atoms for which they are surrogates. In this work we discuss the limitations of the pair potential representation of a colloid system in view of the size polydispersity of that system. The inadequacies of the pair potential representation of a condensed matter system due to the nonzero contribution of the three- and higher-body interactions are generally recognized [3–5]. In nature there is no material with only pair interactions. Even a noble gas, such as argon, is known to have contributions to its properties from the three-body interaction [6]. Similarly, it may be asserted that in nature there is no colloid system that is truly monodisperse. Regardless of this, a pair potential representation is regularly employed in studies of a colloidal matter. The pair potential derived using inversion methods [7,8] is regularly used to extract higher-body correlation functions and the phase behavior of the system. Yet if either a three-body interaction or polydispersity is present, the resulting higher-body correlation functions and the phase diagram cannot be correct. One effect of the three- and higher-body interactions is that the effective pair interaction depends on thermodynamic variables. But even for a single thermodynamic state, the pair potential is not uniquely defined; the pair potential that gives the correct two-point correlation function is different from that which gives the correct excess internal energy [5]. The influence of the triplet attractions on the phase diagram of a suspension of charged particles has been studied in [9]. The density dependence of an effective pair interaction obtained from an experimental Q2D charge-stabilized colloidal system due to a many-body effect is investigated in [10]. The introduction of an appropriate three-body interaction in the same system removes the density dependence in the particle interaction [11]. Issues similar to those exposed in that paper are expected to arise for a polydisperse system.

To date, studies of the influence of polydispersity on system properties have concentrated mainly on phase transitions [12–14]. The coexistence region involves fractionation with components of the mixture distributing unevenly between the phases; the more condensed phase has a higher concentration of smaller particles and the less condensed phase has a higher concentration of larger particles. In addition, broadening of the coexistence region relative to that in the monodisperse limit is observed. The authors in [15] studied the effect of polydispersity on defect concentrations in hard-sphere crystals. They found that the interstitial concentration increases significantly while the concentration of vacancies remains roughly the same. In [16] the authors studied the influence of polydispersity on the elastic constants of hard disks in order to determine the location of the Kosterlitz-Thouless-Halperin-Nelson-Young (KTHNY) melting transition. They found that with increasing polydispersity the dislocation-unbinding transition moved to higher density. But since the solid side of the coexistence region also moves to higher density, the melting mechanism could not be deter-

mined since the difference in onsets of the KTHNY and first-order transitions falls within statistical error.

In this paper we report the results of a study of 2D and Q2D suspensions of spherical colloid particles in which the particle diameters have a prescribed size distribution, $P(\sigma)$. First, we investigate how the polydispersity of colloid particle diameters affects the pair correlation function and the relevant effective pair interaction in the one-component and binary fluid systems. For the binary mixture two scenarios are investigated. In one, the large particles are polydisperse while the small particles are monodisperse. In the other, the large particles are monodisperse while the small-particle component is polydisperse. Next, we investigate the degree of fractionation between compartments of different density for the one-component and binary-fluid systems whose total size distribution corresponds to $P(\sigma)$.

II. METHODS

To carry out the studies mentioned above we devised a method designed to continuously sample a given size distribution function $P(\sigma)$. Before providing a detailed description of this method we first give a short account of other methods that have been used to simulate polydisperse systems.

A. Standard canonical ensemble

In the standard canonical ensemble method a finite polydisperse system is simulated by assigning each particle a diameter from a given size distribution function $P(\sigma)$. Typically, one uses either a random assignment of the diameter of a particle [17] or an assignment of the diameter based on the fixed probability increment (FPI) procedure [18]. In the FPI method the diameter assignment is performed according to the equation

$$(N+1)\int_0^{\sigma_i} d\sigma\, P(\sigma) = i, \tag{1}$$

where N is the number of particle and i is the integer particle index. The FPI assignment method is preferred to random assignment since it yields the most unbiased representation corresponding to a prescribed size distribution $P(\sigma)$. Regardless of the assignment procedure, the canonical ensemble method can only sample a finite set of particle sizes so that size effects in the results are inevitable.

B. Semigrand ensemble

The semigrand ensemble method allows a finite set of particle diameters to fluctuate during the simulation by including particle-resizing moves [19,20]. However, the resulting average size distribution $\langle P(\sigma)\rangle$ cannot be known *a priori* since the fluctuations occur with a prescribed chemical potential difference function $\Delta\mu(\sigma)=\mu(\sigma)-\mu(\sigma_R)$, where $\mu(\sigma_R)$ is the chemical potential of a reference species with diameter σ_R, and must be determined in the simulation.

The semigrand partition function Υ is

$$\Upsilon(N,V,T;\Delta\mu(\sigma)) = \frac{1}{N!\Lambda^{dN}}\int d\sigma^N \prod_{i=1}^{N} e^{\beta\Delta\mu(\sigma_i)} \times \int_V d\mathbf{r}^N\, e^{-\beta U(\mathbf{r}^N,\sigma^N)}. \tag{2}$$

Λ is the thermal de Broglie wavelength and is assumed to be the same for every species, and d is the dimensionality of the system.

C. Inverse Monte Carlo method

The general theme of the inverse Monte Carlo method is to tune the simulation control parameters so as to match some known result obtained earlier via experiment, another simulation, or from an analytic function. The most common application of this method has been the calculation of an effective pair interaction corresponding to a specified structure function or pair correlation function. In this work we use the inverse Monte Carlo technique for just this purpose and we follow the recipe described in [8]. The inverse Monte Carlo method has also been used to determine the chemical potential function $\mu(\sigma)$ for a given size distribution function $P(\sigma)$ [21].

In the inverse Monte Carlo technique the chemical potential function $\mu(\sigma)$ is continuously corrected according to the formula

$$\mu'(\sigma) = \mu(\sigma) - \gamma_k \frac{P_{inst}(\sigma) - P(\sigma)}{P(\sigma)}, \tag{3}$$

where $P_{inst}(\sigma)$ is the instantaneous size distribution function and γ_k is the modification factor for the kth iteration; γ_k is reduced after each iteration. A new iteration cycle starts when the following convergence criterion is satisfied:

$$\frac{1}{M}\sum_{i=1}^{M}\left(\frac{P(\sigma_i) - \overline{P_k}(\sigma_i)}{P(\sigma_i)}\right)^2 \leqslant \xi, \tag{4}$$

where M is the number of grid points, $\overline{P_k}(\sigma)$ is the average size distribution function calculated during iteration k, and ξ is a convergence parameter. When applied to the calculation of the effective pair potential from the pair distribution function, $u_{eff}(r)$ is substituted for $\mu(\sigma)$ and $g_2(r)$ for $P(\sigma)$.

D. $(N,T,V,P(\sigma))$ ensemble method

The inverse Monte Carlo method is, essentially, a simulation in the $(N,T,V,\mu(\sigma))$ ensemble, where $\mu(\sigma)$ is such as to produce a prescribed $P(\sigma)$. To carry out the work described in this paper we have developed a $(N,T,V,P(\sigma))$ ensemble, where $P(\sigma)$ serves as a control parameter. In this method particles in the simulation box are swapped with particles in an infinitely large reservoir with the same density as the simulated system and with size distribution $P(\sigma)$. The swap moves are realized in the following way. A particle i is selected randomly from the simulation box and its diameter is matched with a randomly selected diameter from the size distribution $P(\sigma)$. If the matched diameters satisfy $\sigma > \sigma_i$,

where σ_i is the diameter of a randomly selected particle i and σ is the randomly selected diameter from $P(\sigma)$, then the swap is accepted if no overlap occurs. Otherwise, the move is rejected. A difficulty arises when $\sigma < \sigma_i$ because then σ_i, which is to be swapped with the reservoir particle σ, is larger than this particle and, since instantaneous configurations in the reservoir are unknown, we do not know whether this swapping procedure will produce an overlap or not. To overcome this problem we calculate the swapping (transition) probability $p(\sigma,\sigma')$ between particle sizes σ and σ'. The transition probability $p(\sigma,\sigma')$ satisfies the relation $p(\sigma,\sigma') = p(\sigma',\sigma)$. Here $p(\sigma,\sigma')$ is updated when $\sigma > \sigma_i$, and when $\sigma < \sigma_i$, the move is accepted with probability $p(\sigma,\sigma_i)$.

The same method can be extended to a simulation system with two compartments where particles in different compartments do not interact directly with each other, but are allowed to swap their positions. In addition, each particle is subject to the swap move with the reservoir whose size distribution is $P(\sigma)$. This scenario will necessarily produce a fractionation whenever $\rho_1 \neq \rho_2$ with a constraint $N_1P_1(\sigma) + N_2P_2(\sigma) = (N_1+N_2)P(\sigma)$ and hence corresponds to a system that is divided by an external potential (represented, for example, by a discontinuous step function) into two parts. By employing the two-compartment approach we eliminate the unnecessary effects of the interface. Also, by fixing the number of particles in each compartment rather than allowing a flow of particles between compartments controlled by cost or gain in the potential energy upon exchange, we control the density of each box *a priori*.

III. SYSTEM AND SIMULATION DETAILS

In this paper we study systems with spherical hard-core interactions, where σ denotes the diameter of a disc in the 2D geometry and the diameter of a hard sphere in the Q2D geometry. In the Q2D geometry, the largest particle diameter cannot exceed the length of a plate separation H. For this reason the size distribution function is truncated at diameter size $\sigma = H$. For reasons of comparison, we use the same size distribution function for the strictly 2D system, though the restriction in the z direction has no meaning. For the Q2D system, the wall-particle interaction is a hard interaction.

We have taken for the size distribution function $P(\sigma)$ the Gaussian form

$$P(\sigma) = \frac{1}{\alpha\varepsilon\sqrt{2\pi}} \exp[(\sigma - \overline{\sigma})^2/2\varepsilon^2]. \tag{5}$$

In Eq. (5), $\overline{\sigma}$ is the average particle diameter and α is a normalization constant which arises from truncating a distribution function $P(\sigma)$ beyond $\sigma \geqslant H$ in order to exclude particle diameters larger than the plate separation in the simulation box. The width of the distribution, measured by the parameter ε, characterizes the system polydispersity.

For large particles we have chosen to normalize $P(\sigma)$ as follows:

TABLE I. Author provide caption.

	$\varepsilon = 0.025$	$\varepsilon = 0.05$	$\varepsilon = 0.075$	$\varepsilon = 0.1$
$\rho\overline{\sigma^2} = 0.6$	$\eta = 0.262$	$\eta = 0.264$	$\eta = 0.266$	$\eta = 0.268$
$\rho\overline{\sigma^2} = 0.7$	$\eta = 0.306$	$\eta = 0.308$	$\eta = 0.310$	$\eta = 0.313$
$\rho\overline{\sigma^2} = 0.8$	$\eta = 0.350$	$\eta = 0.352$	$\eta = 0.355$	$\eta = 0.357$

$$\int_{(\overline{\sigma}-H)/2}^{(\overline{\sigma}+H)/2} d\sigma\, P(\sigma) = 1. \tag{6}$$

The upper bound on the permitted range of diameters is taken to be $(\overline{\sigma}+H)/2$ to ensure that all particles can fit into the simulation cell between two confining plates. The lower bound is taken to be $(\overline{\sigma}-H)/2$ to impose symmetry on $P(\sigma)$. We have carried out simulation studies with four distinct size distributions: $\varepsilon = 0.025$, $\varepsilon = 0.05$, $\varepsilon = 0.075$, and $\varepsilon = 0.1$. For the system with the largest polydispersity, $\varepsilon = 0.1$, 4.6% of the particle diameters fall outside the permitted range, and for the system with the next largest polydispersity, $\varepsilon = 0.075$, less than 1% of the particle diameters fall outside the permitted range.

In studying the influence of the polydispersity of small particles on the depletion interaction between large spheres, the bounds of the size distribution of small particles were set at $\overline{\sigma_s} = \pm 3\varepsilon$. Less than 1% of the particle diameters were found to fall outside this region.

Generally, in studies of polydisperse systems, results are reported for the packing fraction defined by

$$\eta = \frac{\pi}{6}\frac{N}{V}\int d\sigma\, P(\sigma)\sigma^3. \tag{7}$$

In this study we report our results for large particles in terms of the number density $\rho = N/A$ (A denotes the area), which, unlike the packing fraction, is a measurable experimental quantity. For the sake of completeness we provide a table (Table I) containing values of the packing fraction for a given ρ and ε. For small particles, on the other hand, our results are reported in terms of the packing fraction, which is a more suitable quantity for studies of the depletion interaction. The packing fraction is defined as $\eta_s = \pi\sigma_s^3 N_s/6HA$.

All simulations for the single-component system were performed in the $(N,T,A,H,P(\sigma))$ ensemble, where A is the area and H is the height of the cell. The number of particles was set to $N = 504$, unless otherwise specified. The aspect ratio of the area of the periodic box was $7:4\sqrt{3}$. The two-compartment scenario, in addition, allowed swaps between compartments which were defined by $N_1 = N_2 = 504$, $H_1 = H_2$, and $\rho_1 \neq \rho_2$.

For binary system simulations we used the $(N,z_s,T,A,H,P(\sigma))$ ensemble, where z_s is the fugacity of the small particles. In order to match z_s to a desired density ρ_s^r we used the fundamental relation $\rho_s^r \exp(\beta\mu_s^{ex}) = z_s$ where μ_s^{ex} is the excess chemical potential of the small spheres. The Carnahan-Starling equation of state was used to calculate μ_s^{ex}, since that equation of state is very accurate in the density regime of interest. In the two-compartment configuration

ρ_s^r is the same in each compartment. All of the binary colloid systems studied had a diameter ratio $q=0.3$, where $q=\sigma_s/\overline{\sigma}$. This order of q is within the range commonly used in experimental studies, and it facilitates simulation calculations since as q gets smaller the number of particles needed grows rapidly.

The swapping probability $p(\sigma,\sigma')$ needed for application of the acceptance criterion when a particle switches to a smaller diameter was stored in a two-dimensional array p_{ij}. That array was divided into 200×200 bins. Each element of the p_{ij} array was initially set to some finite value so as not to exclude any swap. Each time a particle was switched to a larger diameter, p_{ij} was updated. When the new particle diameter was smaller than the old particle diameter, the swap was accepted with a probability based on the appropriate p_{ij}. When the two-compartment scenario was used, a particle to be swapped with the reservoir was selected randomly from the total number of particles, N_1+N_2.

The equilibration cycle we used had three stages. The first stage started with a random assignment of diameters according to $P(\sigma)$. In this stage particle swaps with the reservoir were prohibited and the system was allowed to warm up. For the two-compartment setup particle swaps between compartments were permitted. In the second stage the updating procedure for p_{ij} was started. Only in the third stage were particle swaps with the reservoir allowed.

All studies of the Q2D system were carried out with $H=1.2\overline{\sigma}$, which roughly corresponds to plate separations found in experimental systems [22]. Accordingly, we use $H=1.2\overline{\sigma}$ to truncate the size distribution function for both the Q2D and strictly 2D geometries. For the Q2D case the symbol r always indicates the two-particle separation projected on the xy plane $[r=\sqrt{(x_2-x_1)^2+(y_2-y_1)^2}]$.

IV. SIMULATION RESULTS

A. Testing the $(N,T,V,P(\sigma))$ ensemble

To demonstrate sample-to-sample fluctuations inherent to the canonical ensemble method we show in Fig. 1(a) a number of pair correlation functions, $g_2(r)$, calculated for the same system, but for different sets of particle diameters selected randomly from $P(\sigma)$. The number of particles is $N=504$ and the system is strictly 2D with $\rho\overline{\sigma^2}=0.8$. We carried out the simulations for a system size up to $N=8064$ and we found that the sample-to-sample fluctuations disappear for $N=2016$. The results for $N=2016$ and higher can be assumed to be equivalent to the exact results for the continuous size distribution. In Fig. 1(b) we compare the $g_2(r)$ obtained using different methods. For the standard canonical ensemble we used two sets of particles: one selected randomly with $N=8064$ and the other selected using the FPI assignment method [Eq. (1)] with $N=504$. The sample size of the $(N,T,V,P(\sigma))$ ensemble was $N=504$. All of the calculated pair correlation functions are nearly the same. The FPI method gives very good results despite the finite sampling of the particle sizes.

Figure 2(a) shows the measured average size distribution $\langle P(\sigma)\rangle$ using the $(N,T,V,P(\sigma))$ ensemble for $\varepsilon=0.1$. Here

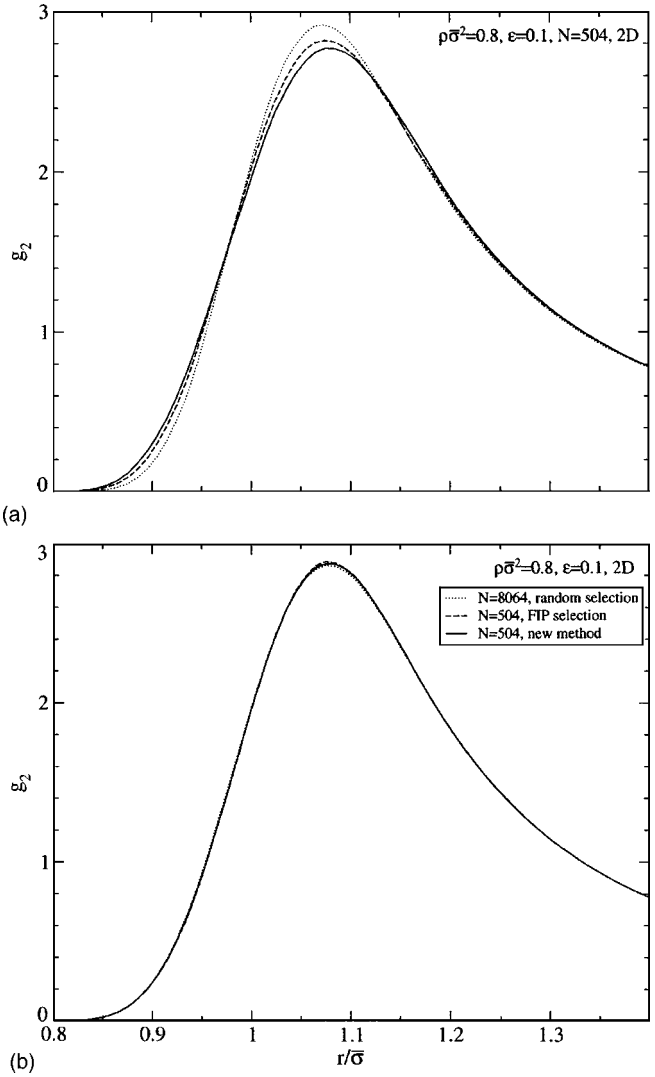

FIG. 1. The pair correlation functions $g_2(r)$ for the number density $\rho\overline{\sigma^2}=0.8$ and the 2D geometry, calculated using different methods and for different system sizes.

$\langle P(\sigma)\rangle$ is indistinguishable from $P(\sigma)$ given in Eq. (5). Note that $P(\sigma)$ is truncated at $H=1.2\overline{\sigma}$ to facilitate a comparison with the Q2D geometry. Figure 2(b) shows the measured swapping probability $p(\sigma,\sigma')$ for the same system. Cast in the form $p(\sigma,|\sigma-\sigma'|)$, the swapping probability is 1 whenever $|\sigma-\sigma'|=0$ and decays exponentially with increasing $|\sigma-\sigma'|$.

B. Effective interaction between polydisperse hard spheres

Figure 3 shows the dependence of $g_2(r)$ and $u_{eff}(r)$ on the colloid polydispersity for a strictly 2D system at number density $\rho\overline{\sigma^2}=0.8$. The effective pair potential $u_{eff}(r)$ was calculated using the inverse Monte Carlo method [8] as described in Sec. II C. As ε increases, the peaks of the pair correlation function become more rounded. This is expected because the possible particle separations where the hard-core interaction occurs, $\sigma_{12}=(\sigma_1+\sigma_2)/2$, spread around the value

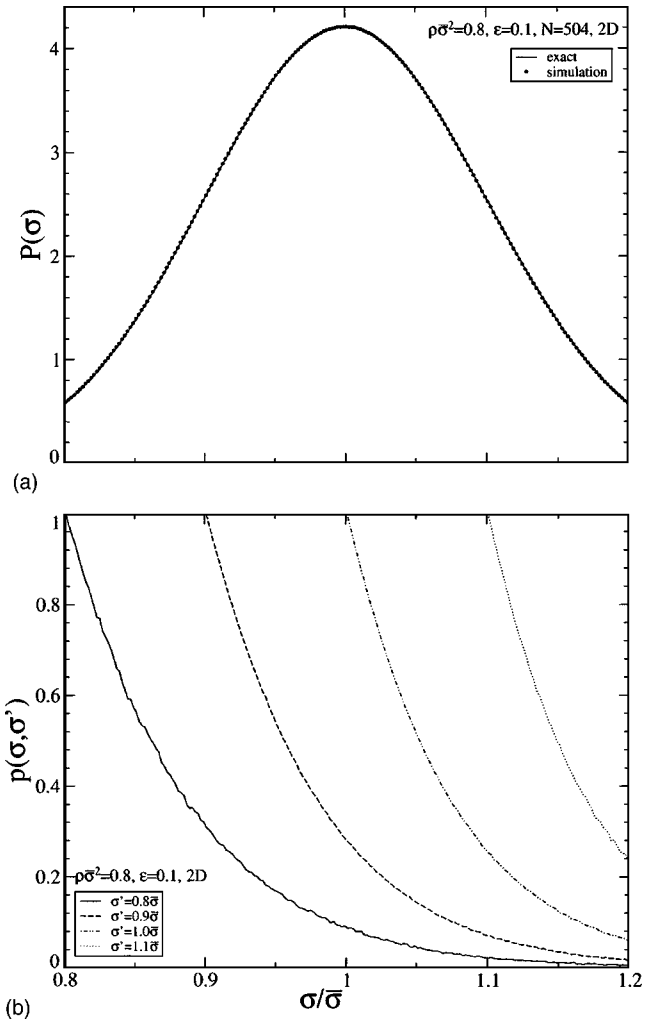

FIG. 2. The size distribution function $P(\sigma)$ and the swapping probability $p(\sigma,\sigma')$ calculated in the $(N,T,V,P(\sigma))$ ensemble for the number density $\rho\overline{\sigma}^2=0.8$ and the 2D geometry. In (a), $P(\sigma)$ is truncated at $H=1.2\overline{\sigma}$ to facilitate a comparison with the Q2D geometry.

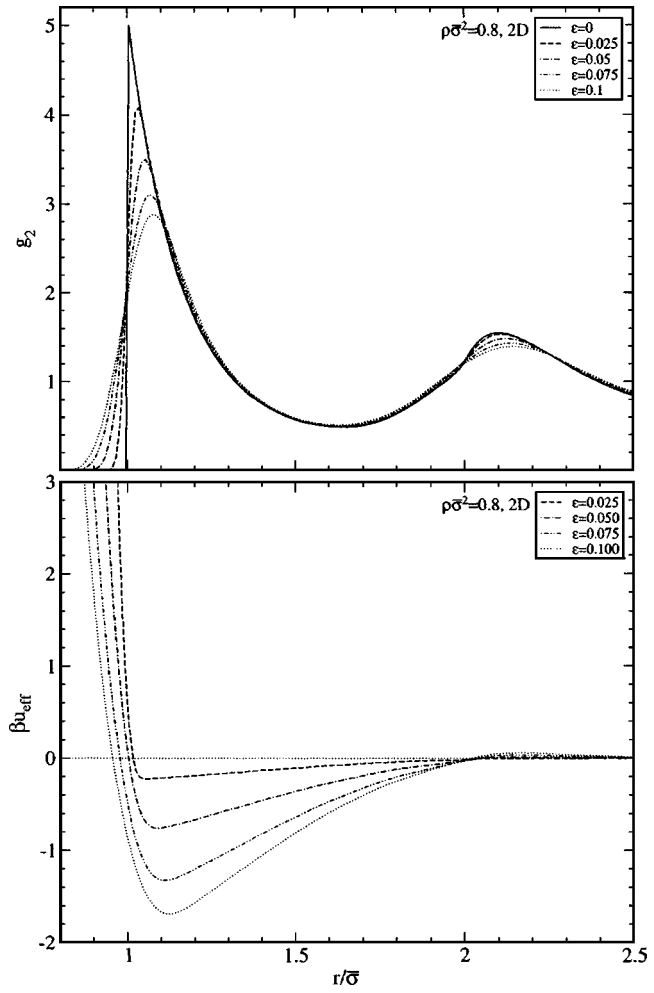

FIG. 3. The pair correlation functions $g_2(r)$ and the corresponding effective pair potentials $u_{eff}(r)$ for various polydispersities for the number density $\rho\overline{\sigma}^2=0.8$ and the 2D geometry.

$\overline{\sigma}$. This creates the impression of a soft repulsion with ε being a softness parameter. On the other hand, the attractive component of the effective pair interaction could not be inferred directly from the pair correlation function. This attraction suggests that the peaks of the pair correlation function are larger than the effective soft repulsion alone would produce. The attractive component of the effective interaction increases with increasing ε. The complete effective pair potential is an oscillating function whose period corresponds to the oscillations in the pair correlation function of the polydisperse system. However, the effective interactions beyond the second peak are negligible and the range of the effective interaction vanishes beyond $r\approx 2\overline{\sigma}$.

To ensure that the effective attraction due to polydispersity is not an artifact of the Gaussian distribution, but is a general feature of polydispersity, we have also carried out simulations for polydispersities characterized by a uniform distribution function

$$P_f(\sigma)=\begin{cases}1/2\varepsilon_f, & \overline{\sigma}-\varepsilon_f\leqslant\sigma\leqslant\overline{\sigma}+\varepsilon_f,\\ 0, & \text{otherwise}.\end{cases} \tag{8}$$

In Eq. (8), ε_f is a parameter that controls the width of the distribution. We found that the calculated effective pair potentials for the uniform distribution exhibit features that are qualitatively the same as those found for a colloid system with a Gaussian size distribution.

Next, we investigate the density dependence of the polydispersity effects by plotting in Fig. 4 the effective pair interaction $u_{eff}(r)$ for a number of densities for $\varepsilon=0.05$ and $\varepsilon=0.1$ in a strictly 2D system. $u_{eff}(r)$ shows a strong density dependence; at low density, the attractive part of the effective potential almost completely disappears and only the effective soft repulsion remains.

The pair correlation function has the following exact representation when $\rho\to 0$:

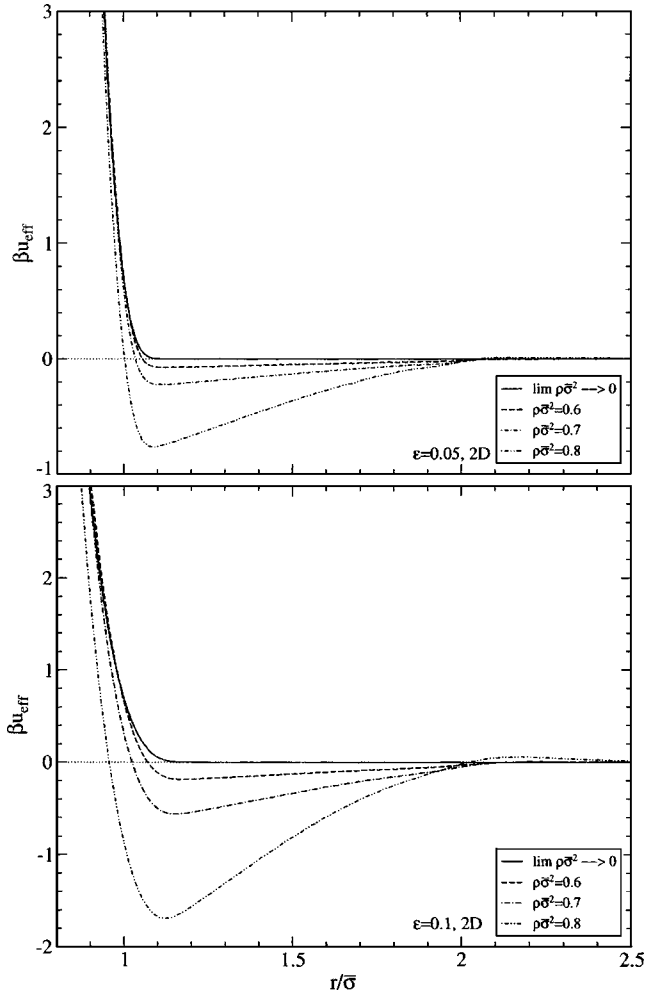

FIG. 4. The density dependence of the effective pair interactions for $\varepsilon=0.05$ and $\varepsilon=0.1$ in the 2D geometry. The dilute limit was calculated both from Eqs. (9) and (10) and from the simulation at density $\rho\overline{\sigma^2}=0.01$. Both results give the same results.

$$\lim_{\rho\to 0} g_2(r;\rho) = \int d\sigma_1 \int d\sigma_1\, P(\sigma_1)P(\sigma_2)\,\theta(2r-\sigma_1-\sigma_2), \tag{9}$$

where $\theta(r-a)$ is the unit step function. The effective pair interaction in this limit is

$$\lim_{\rho\to 0} \beta u_{eff}(r;\rho) = \lim_{\rho\to 0}[-\ln g_2(r;\rho)]. \tag{10}$$

We found that the effective pair potential calculated at $\rho\overline{\sigma^2}=0.01$ agrees within statistical error with the effective pair potential in the dilute limit given by Eq. (10). In Fig. 4 we plot the effective pair interaction for $\varepsilon=0.05$ and 0.1 for $\rho\to 0$. The effective attraction disappears as the density approaches zero. However, the effective soft repulsion remains even in the zero-density limit. This result shows that unlike the case of many-body interactions, polydispersity effects cannot be eliminated even in the limit $\rho\to 0$ and a true pair interaction for the polydisperse system does not exist.

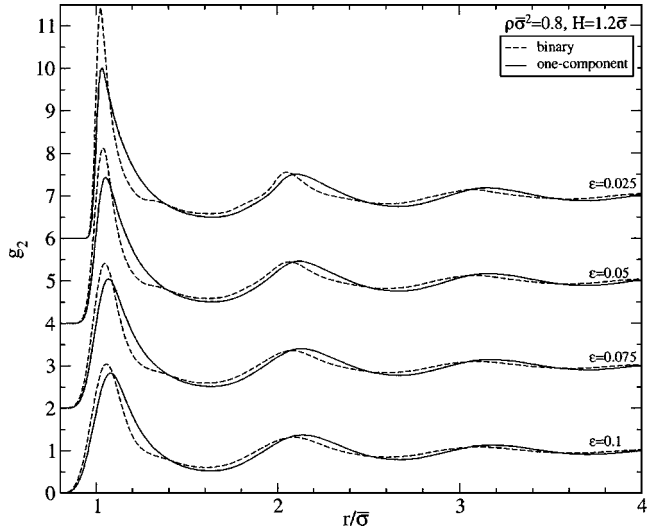

FIG. 5. The pair correlation functions $g_2(r)$ for the one-component and binary system at density $\rho\overline{\sigma^2}=0.8$ for various ε. In the binary system small particles are monodisperse and correspond to parameters $q=0.3$ and $\eta_s^r=0.19$.

Finally, we shift our focus of study to a more realistic Q2D geometry with plate separation $H=1.2\overline{\sigma}$. In experimental studies, the plate separation is comparable with this value [22]. A comparison of the effective pair interaction between the strictly 2D and Q2D systems indicates that the out-of-plane motion when $H=1.2\overline{\sigma}$ produces only very small changes which include a slight softening of the effective repulsion and a slight decrease in the depth of the attractive well. Otherwise, the out-of-plane motion makes an insignificant contribution to our results. Note that in the Q2D geometry r always refers to the xy projection of the particle separation.

C. Effective interaction between polydisperse hard spheres immersed in a monodisperse small-particle fluid

We now investigate the influence of the colloid polydispersity on the colloid-colloid depletion interaction due to introduction of a second colloid species with a monodisperse diameter distribution. The size ratio of the binary mixture is $q=0.3$ and the chemical potential of the small particles corresponds to small-particle reservoir packing fraction $\eta_s^r=0.19$.

Figure 5 shows the change in the large-particle pair correlation function at density $\rho\overline{\sigma^2}=0.8$ for different values of ε when the second component of small particles is introduced. For all polydispersities the amplitude of the first peak of the pair correlation function increases and the second and subsequent peaks shift to smaller separations, indicating an attractive depletion interaction, in agreement with the findings for the monodisperse system.

Figure 6 shows the depletion potential $u_{dep}(r)$, defined as the difference between the effective pair potential of the binary and one-component systems. As in the one-component case, the effective depletion pair potential displays a strong dependence on the large-particle density and on the degree of

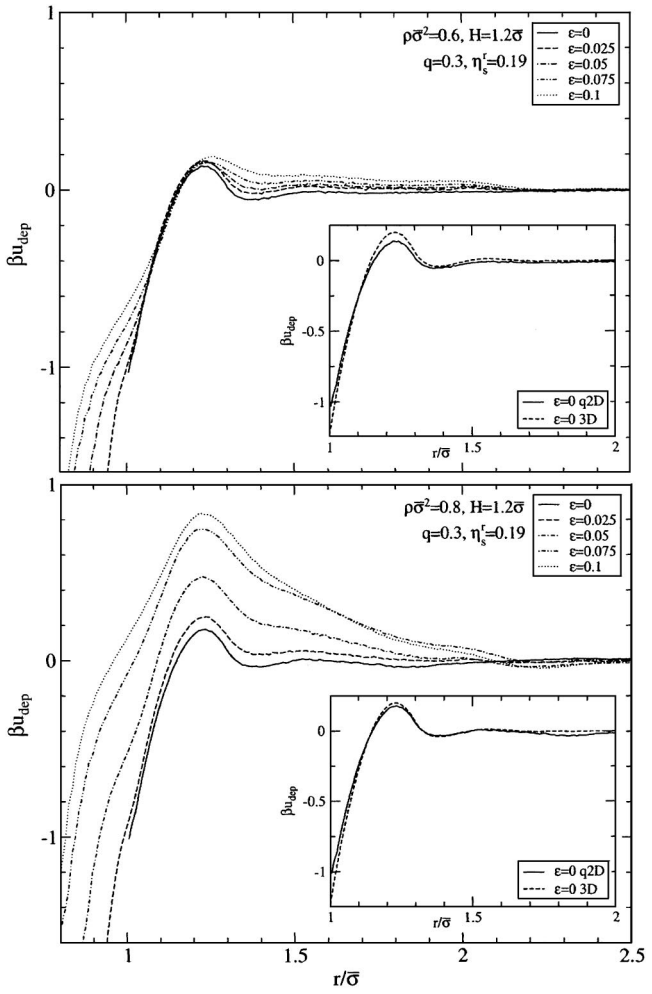

FIG. 6. The depletion pair interactions $u_{dep}(r)$ defined as the difference between $u_{eff}(r)$ of the binary and one-component systems for density $\rho\overline{\sigma}^2=0.6$ and $\rho\overline{\sigma}^2=0.8$ and various ε. In the binary system small particles are monodisperse and correspond to parameters $q=0.3$ and $\eta_s^r=0.19$. In the inset we compare the depletion pair interaction of monodisperse systems for the Q2D system with plate separation $H=1.2\overline{\sigma}$ and the 3D system.

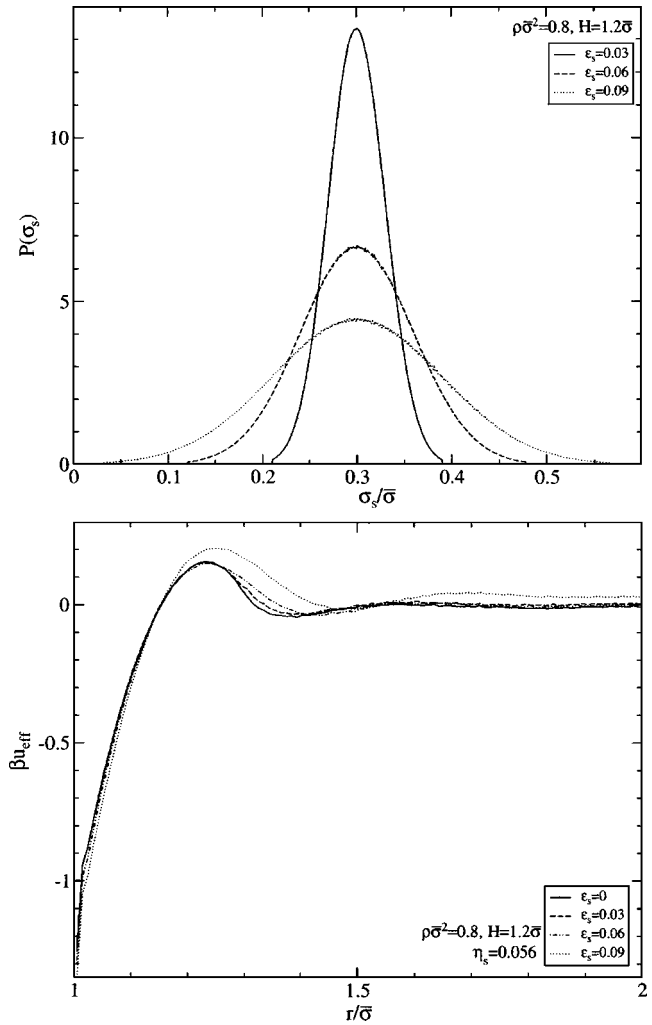

FIG. 7. The effective pair interactions for monodisperse large particles in a sea of small polydisperse particles together with the small-particle diameter distributions $P(\sigma_s)$ are shown in the upper graph. The number of small particles in the system gives the packing fraction of small particles, $\eta_s=0.056$.

polydispersity. At density $\rho\overline{\sigma}^2=0.6$ there are only very small ε-dependent changes to the depletion pair potential. The polydispersity-dependent feature in the depletion pair potential is the repulsive barrier which extends from particle separation $\sim 2\overline{\sigma}$ and is peaked at particle separation $\sim 1.25\overline{\sigma}$. In the inset of Fig. 6 we compare the depletion pair potential in the monodisperse limit for the confined system with plate separation $H=1.2\overline{\sigma}$ and for the 3D homogeneous system. The difference between the two potentials is very small and includes the slight increase in the repulsive barrier and in the depth of the attractive well for the 3D homogeneous depletion pair potential.

D. Effective interaction between monodisperse hard spheres immersed in a polydisperse small-particle fluid

In this section we investigate the influence of polydispersity of the small particles on the depletion interaction between large colloid particles while keeping the large particles in the monodisperse limit. We carried out this study using the $(N,N_s,T,A,H,P(\sigma_s))$ ensemble, where N_s is the number and $P(\sigma_s)$ is the particle diameter distribution of small particles. The number of small particles depended on the particular form of $P(\sigma_s)$ and was such as to give a desired packing fraction η_s. The target η_s was the average small-particle packing fraction of the monodisperse binary mixture with parameters $q=0.3$ and $\eta_s^r=0.19$. The Gaussian distribution for the small particles had the average diameter set to $\overline{\sigma_s}=0.3$ and the plate separation was set to $H=1.2\overline{\sigma}$.

In Fig. 7 we plot the small-particle size distributions $P(\sigma_s)$ for polydispersities corresponding to $\varepsilon_s=0.03$, $\varepsilon_s=0.06$, and $\varepsilon_s=0.09$, together with the resulting effective pair potentials for the large particles. In this case, the effective pair potential is equivalent to the depletion pair potential since in the monodisperse limit the effective pair potential of the pure large-particle system is a hard-core interaction. $P(\sigma_s)$ is trimmed at $\overline{\sigma_s}=\pm 3\varepsilon_s$. The effect of the slight devia-

tion from the strict hard-core interaction due to the out-of-plane motion was found to be negligible. The depletion potential shows amazingly little variation with increasing ε_s. The attractive part of the depletion potential is essentially unchanged and only the repulsive peak seems to be affected at all when the polydispersity is changed. The repulsive peak slightly increases in magnitude and its range is extended to larger particle separations as the polydispersity increases. This is essentially in agreement with the results reported in [23] where the depletion potential between two large hard spheres immersed in the polydisperse 3D sea of small particles was calculated using the density functional theory. At constant packing fraction of small particles, polydispersity was found to have little effect on the depletion attraction. The repulsive barrier was found to be extended with increasing polydispersity, but unlike our results, its magnitude was found to be reduced.

Studies of the effective pair potential between large spheres immersed in a multicomponent hard-sphere fluid show a rich structure in the effective pair potential due to the presence of different diameter sizes of small spheres [24]. In our case, the background fluid into which large spheres are immersed is polydisperse and so the number of species constituting the background fluid is infinite. As a result, we do not observe an enrichment in the structure. The range remains unchanged, which is the result of keeping the average small particle size constant. The magnitude of the effective pair interaction remains roughly constant due to keeping the small-particle packing fraction fixed at one value for all ε_s.

E. Fractionation between the two-compartment polydisperse hard-sphere fluid

In this section we show the results from simulations with two compartments. The plate separation in each compartment was set to $H=1.2\overline{\sigma}$. Each compartment had the same number of particles, but different density. As particles were swapped between samples of different density, the total size distribution $P_1(\sigma)/2+P_2(\sigma)/2=P(\sigma)$ was constrained to be the same. The system simulated in this way provides a representation of a possible experimental setup where in the same sample clusters of different density and size are present. This situation occurs, for example, in the coexistence region. As a result, fractionation occurs between different phases, where the more condensed phase prefers smaller particles [12–14]. In our double-compartment setup, the division into different density regions does not result from phase separation, but rather from the intervening external potential. In an experiment, such an external potential could be an electric field acting on charged colloidal particles. Another source of the density variation, which is more relevant for the system we attempt to reproduce, is caused by the varying plate separation throughout the experimental cell. The chemical potential being equal everywhere in the sample, the density should vary with varying plate separation since a larger plate separation has more volume to accommodate more particles. As the plate separation decreases, fewer particles can fit between the plates, and in the limit $H\rightarrow\sigma$, the density approaches zero (assuming a monodisperse limit where the particle diameter is σ).

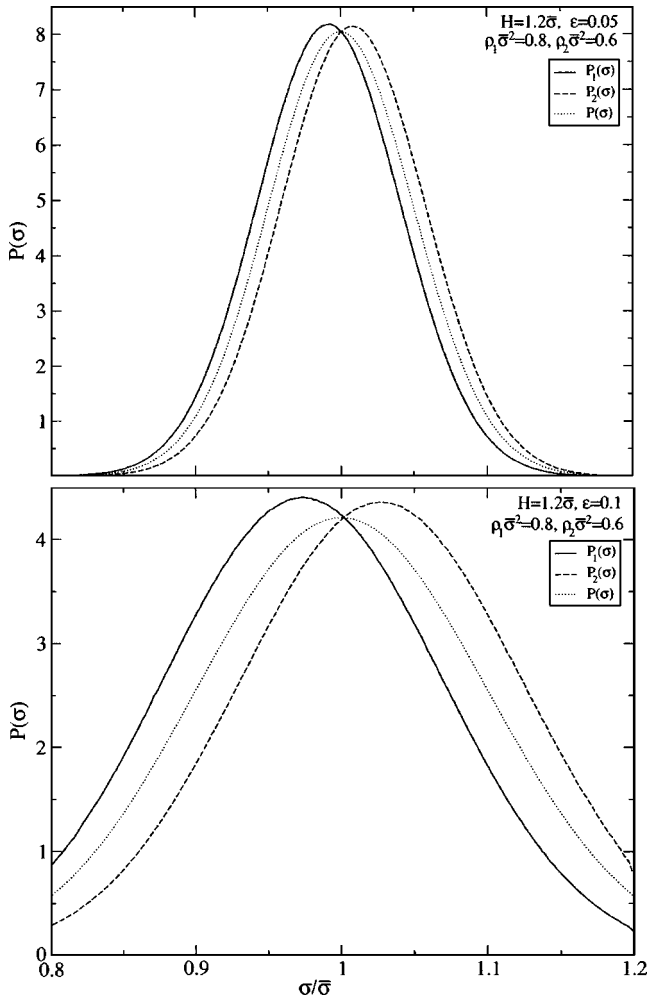

FIG. 8. The size fractionation in the two-compartment simulation with densities $\rho_1\overline{\sigma^2}=0.8$ and $\rho_2\overline{\sigma^2}=0.6$ in the Q2D geometry.

Figure 8 shows the effect of fractionation between two compartments with density $\rho_1\overline{\sigma^2}=0.8$ and $\rho_2\overline{\sigma^2}=0.6$ for polydispersity $\varepsilon=0.05$ and $\varepsilon=0.1$. As expected, the susceptibility to fractionate increases with increasing polydispersity and the size distribution shifts to smaller particles for the higher-density region and vice versa. Figure 9 displays the mean particle diameter $\langle\sigma\rangle$ in two compartments with the density of the first compartment fixed at $\rho_1=0.8$ and the density of the second compartment changing between 0.5 and 0.8. As the density difference between two compartments increases, so does the extent of fractionation. The rate of fractionation with increasing density difference is greatest when the density difference is zero and decreases monotonically with increasing density difference.

F. Fractionation between the two-compartment polydisperse hard spheres immersed in a monodisperse small-particle fluid

We now investigate the influence of the depletion interaction on the fractionation effect of the polydisperse colloid system. The chemical potential of small particles and the plate separation are the same in each compartment. The

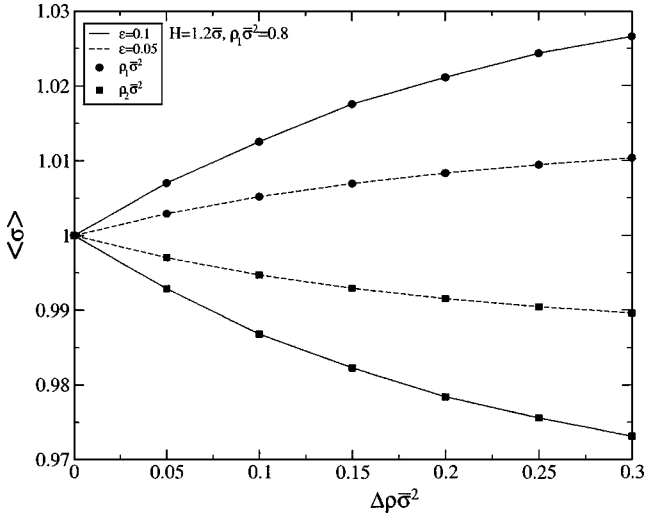

FIG. 9. The average particle diameter $\langle\sigma\rangle$ for the two-compartment simulation as a function of a density gap between two compartments ($\Delta\rho=\rho_1-\rho_2$, where ρ_1 and ρ_2 denote the density of compartments 1 and 2, respectively). The density gap is manipulated by varying the density of the second compartment; the density of the first compartment is always fixed at $\rho_1\overline{\sigma^2}=0.8$. The circles represent data points for compartment 1 and squares represent data points for compartment 2.

packing fraction of the small particles is set at $\eta_s^r=0.19$ and the plate separation is set at $H=1.2\overline{\sigma}$. Figure 10 compares the size distribution in each compartment of the one-component and binary systems at densities $\rho_1\overline{\sigma^2}=0.8$ and $\rho_2\overline{\sigma^2}=0.6$. The depletion interaction arising from the small particles has a defractionation influence on the double-compartment system. To further demonstrate the quenching influence of the depletion interaction on the fractionation process in Fig. 11(a) we plot the average particle size in each compartment as a function of $\rho_2\overline{\sigma^2}$ when $\rho_1\overline{\sigma^2}$ is fixed at $\rho_1\overline{\sigma^2}=0.8$ for the one-component and binary systems. Figure 11(b) also displays

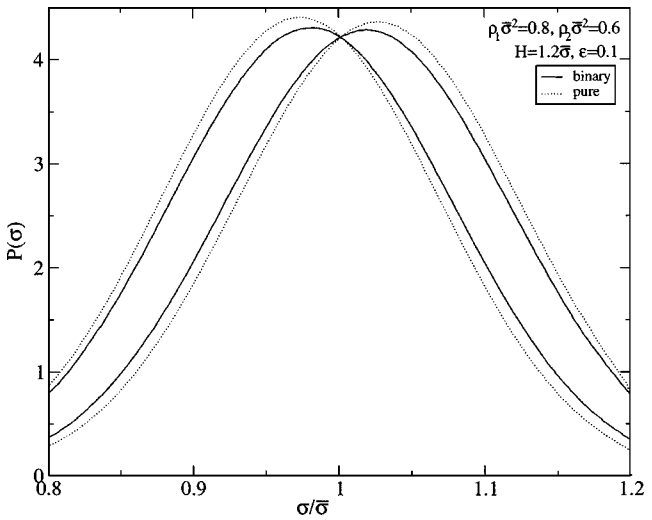

FIG. 10. The comparison of the size fractionation in the two-compartment simulation for the one-component and binary systems. The small particles in the binary mixture are monodisperse and correspond to the size ratio $q=0.3$ and $\eta_s^r=0.19$.

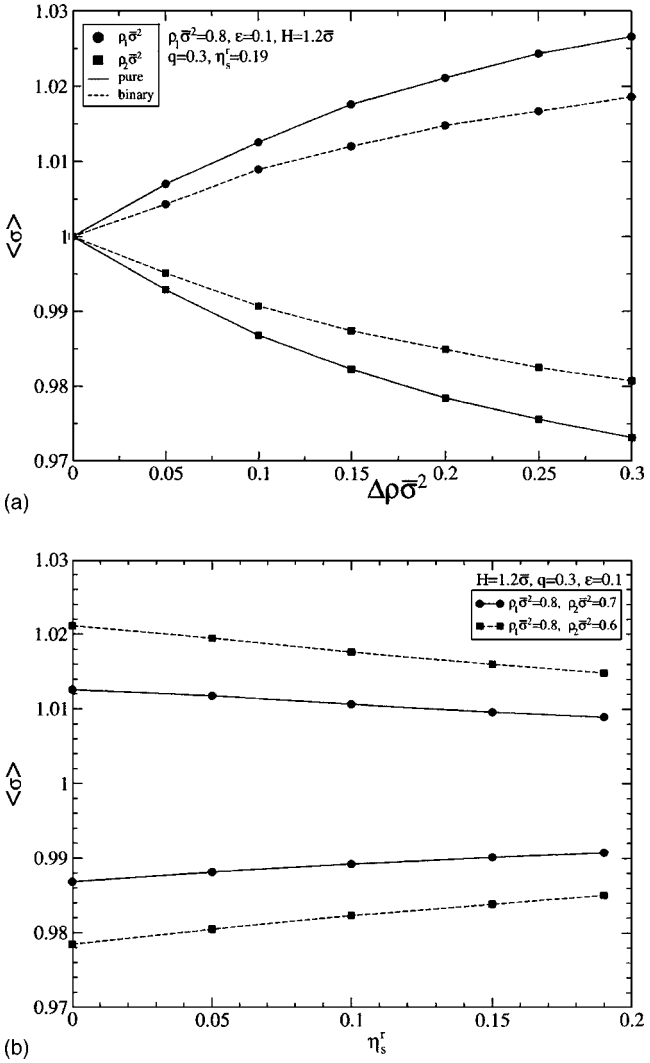

FIG. 11. The average particle diameter $\langle\sigma\rangle$ for the two-compartment simulation as a function of (a) a density gap between two compartments ($\Delta\rho=\rho_1-\rho_2$, where ρ_1 and ρ_2 denote the density of the compartment 1 and 2, respectively) and (b) η_s^r. Small particles are monodisperse with size ratio $q=0.3$. In (a) the density gap is manipulated by varying the density of the second compartment; the density of the first compartment is always fixed at $\rho_1\overline{\sigma^2}=0.8$.

the average particle size, but now for fixed densities of two compartments, as a function of η_s^r. The addition of small particles into the double-compartment system reduces the fractionation effect, but it is hard to tell whether at very high density of small particles the fractionation completely disappears before the binary system undergoes a phase transition.

To explain this phenomenon, we note that the predominant part of the depletion interaction consists of an attractive component and, as a result, the large colloid particles more often stay together in tight cluster aggregates. This behavior can be inferred from the pair correlation functions (Fig. 5) where the primary peak increases and the correlation length decreases with increasing density of small particles. This process puts particles in both compartments on a similar footing, since both compartments develop cluster structures, and so it becomes more difficult for the compartment with

higher density to trade smaller particles with a lower-density compartment.

V. CONCLUSION

The calculations reported in this paper were undertaken to better understand the influence of polydispersity on the effective pair potential in Q2D colloid assemblies (with extension to 2D colloid assemblies). The results of the studies reported in this paper suggest that at high density colloid polydispersity is a dominant artifact that generates an apparent attractive interaction in addition to soft repulsion between what should be hard-sphere colloid particles. The range of the attractive well is $2\overline{\sigma}$. As the density decreases, the effective attraction grows smaller and disappears completely once the dilute limit is reached. However, the effective soft repulsion remains even in the dilute limit, and unlike the case when three- and higher-body interactions are present, polydispersity effects can never be completely eliminated.

In studies of the effective interaction between large polydisperse colloid particles in a medium with small monodisperse colloid particles, the polydispersity generates a repulsive soft potential with range $2\overline{\sigma}$. As the density decreases, the repulsion grows smaller, but never completely disappears. In studies of the effective interaction between large monodisperse colloid particles in a medium with small polydisperse colloid particles, the polydispersity effects are very small when the packing fraction of small particles [Eq. (7)] is kept constant. The main effects are the increase and extension of the repulsive barrier.

We conclude that the derivation of an effective colloid-colloid interaction by inversion of experimental pair correlation function data must account for polydispersity in the distribution of colloid diameters. Without that correction it is not possible to test the theory of the depletion interaction or to fully understand how phase boundaries change under the influence of a depletion interaction.

ACKNOWLEDGMENTS

This research was supported by a grant from the National Science Foundation (No. CHE-9977841). We have also benefitted from the support of the National Science Foundation funded MRSEC Laboratory at the University of Chicago.

[1] W. G. McMillan and J. E. Mayer, J. Chem. Phys. **13**, 276 (1945).
[2] D. Frydel and S. A. Rice, Phys. Rev. E **68**, 061405 (2003).
[3] J. A. Barker, D. Henderson, and W. R. Smith, Mol. Phys. **17**, 579 (1969).
[4] J. S. Rowlinson, Mol. Phys. **52**, 567 (1984).
[5] A. A. Louis, J. Phys.: Condens. Matter **14**, 9187 (2002).
[6] B. M. Axilrod and E. Teller, J. Chem. Phys. **11**, 299 (1943).
[7] L. Reatto, D. Levesque, and J. J. Weis, Phys. Rev. A **33**, 3451 (1986).
[8] N. G. Almarza and E. Lomba, Phys. Rev. E **68**, 011202 (2003).
[9] A. Hynnien, M. Dijkstra, and R. van Roij, J. Phys.: Condens. Matter **15**, S3549 (2003).
[10] M. Brunner, C. Bechinger, W. Strepp, V. Lobaskin, and H. H. von Grünberg, Europhys. Lett. **58**, 926 (2002).
[11] C. Russ, M. Brunner, C. Bechinger, and H. H. von Grünberg, Europhys. Lett. **69**, 468 (2005).
[12] D. A. Kofke and P. G. Bolhuis, Phys. Rev. E **54**, 634 (1996).
[13] D. A. Kofke and P. G. Bolhuis, Phys. Rev. E **59**, 618 (1999).
[14] N. B. Wilding and P. Sollich, Europhys. Lett. **67**, 219 (2004).
[15] S. Pronk and D. Frenkel, J. Chem. Phys. **120**, 6764 (2004).
[16] S. Pronk and D. Frenkel, Phys. Rev. E **69**, 066123 (2004).
[17] D. Frenkel, R. J. Vos, C. G. de Kruif, and A. Vrij, J. Chem. Phys. **84**, 4625 (1986).
[18] L. Santen and W. Krauth, e-print cond-mat/0107459.
[19] D. A. Kofke and E. D. Glandt, J. Chem. Phys. **87**, 4881 (1987).
[20] D. A. Kofke and E. D. Glandt, Mol. Phys. **64**, 1105 (1988).
[21] N. B. Wilding, J. Chem. Phys. **119**, 12163 (2003).
[22] B. Cui, B. Lin, and S. A. Rice, J. Chem. Phys. **119**, 2386 (2003).
[23] D. Goulding and J. P. Hansen, Mol. Phys. **865**, 99 (2001).
[24] D. Henderson, D. T. Wasan, and A. Trokhymchuk, J. Chem. Phys. **119**, 11989 (2003).